Journal of the Meteorological Society of Japan

EARLY ONLINE RELEASE

This is a PDF of a manuscript that has been peer-reviewed and accepted for publication. As the article has not yet been formatted, copy edited or proofread, the final published version may be different from the early online release.

This pre-publication manuscript may be downloaded, distributed and used under the provisions of the Creative Commons Attribution 4.0 International (CC BY 4.0) license. It may be cited using the DOI below.

The DOI for this manuscript is

DOI:10.2151/jmsj.2019-054

J-STAGE Advance published date: July 5th, 2019

The final manuscript after publication will replace the preliminary version at the above DOI once it is available.

Role of Local Air-Sea Interaction in a Significant Correlation of Convective Activity in the Western Pacific Warm Pool between June and August

Feng XUE[1]

International Center for Climate and Environment Sciences, Institute of Atmospheric Physics, Chinese Academy of Sciences, Beijing, 100029, China

and

Fangxing FAN

International Center for Climate and Environment Sciences, Institute of Atmospheric Physics, Chinese Academy of Sciences, Beijing, 100029, China

June 16, 2019

---

1) Corresponding author: Feng Xue, International Center for Climate and Environment Sciences, Institute of Atmospheric Physics, Chinese Academy of Sciences, Beijing, 100029, CHINA

Email: fxue@lasg.iap.ac.cn

Tel: +86-10-82995282

Fax: +86-10-82995123

Abstract

Based on the monthly outgoing longwave radiation (OLR) data from 1979 to 2013, a significant correlation of convective activity over the western Pacific warm pool between June and August is detected while there are no significant correlations between June and July and between July and August. The analysis results indicate that consistent anomalies in June and August usually occur during the years with strong warm pool convection. Moreover, two prerequisites are necessary for this consistent anomaly, i.e., a higher sea surface temperature (SST) over the warm pool during the preceding spring and a relatively weak El Niño and Southern Oscillation (ENSO). An analysis based on the selected typical years indicates that convection in June tends to enhance when the warm pool SST is higher in the spring. The enhanced convection, in turn, reduces the solar insolation and local SST and consequently suppresses convection in July. In contrast to June, the local SST tends to increase due to the suppressed convection in July. Accordingly, the warm pool convection in August is subsequently enhanced again. In this process, the local air-sea interaction plays a major role in regulating SST anomalies from June to August and forming the consistent warm pool convection anomalies in June and August. There are additional complications in understanding intraseasonal variation in the warm pool convection from June to August as related to the ENSO forcing. During strong El Niño decaying years (e.g., 1998), the warm pool convection is suppressed with consistent positive OLR anomalies from June to August, implying that the El Niño forcing contributes to the significant positive correlation of convective activity between June and August. During moderate El Niño decaying years (e.g., 2007), however, the convection anomaly in June is opposite to that in August. In general, the local air-sea interaction effect plays an essential role in the significant correlation of convective activity between June and August, though this correlation also depends on the intensity of the El Niño forcing.

Key words warm pool convection; positive correlation; local air-sea interaction; ENSO

1. Introduction

During boreal summers, large-scale convective cloud clusters are observed from South China Sea to the east of the Philippines; these clusters are often referred to as the western Pacific warm pool convection. Climatologically, the warm pool convection begins to gradually intensify after the onset of the South China Sea summer monsoon in late May (Tao and Chen, 1987; Lau and Yang, 1997; Ding and Liu, 2001). In late July, the warm pool convection suddenly shifts northeastward, thus signaling the onset of the tropical western Pacific summer monsoon. Specifically, this shift leads to an anomalous anticyclone in the subtropical East Asia and the termination of the Meiyu or Baiu seasons from the Yangtze River basin to Japan (Ueda et al., 1995; Wu, 2002). As major characteristics of intraseasonal variation of the East Asian summer monsoon (EASM), the two northward jumps of the western Pacific subtropical high (WPSH) occurring in mid-June and late July are also associated with the enhanced warm pool convection (Su and Xue, 2010).

Many observational studies have shown that the interannual variability of the EASM is also influenced by the warm pool convection. In general, the enhanced (suppressed) convection tends to be associated with an anticyclonic (cyclonic) anomaly in East Asia generated by a Rossby wave train propagating northward (Nitta, 1987; Tsuyuki and K. Kurihara, 1989). This teleconnection pattern between the tropical western Pacific and East Asia is referred to as the Pacific-Japan pattern (Nitta, 1987). Lu (2001a) further showed that the zonal displacement of the WPSH is affected by the warm pool convection. The enhanced (suppressed) convection can excite a low-level cyclonic (anticyclonic) anomaly in the subtropical western Pacific, leading to the eastward retreat (westward

extension) of the WPSH. Therefore, the warm pool convection plays a crucial role in the EASM variability on intraseasonal and interannual timescales; thus, understanding the mechanism for the warm pool convection is of considerable importance for EASM predictions.

The warm pool convection is generally recognized as being influenced by both local and remote SST anomalies that are regulated by the El Niño and Southern Oscillation (ENSO) phase (Lau and Nath, 2009; Wu et al., 2010; Lu and Lu, 2014). In La Niña years when a local SST is higher, the warm pool convection tends to enhance through local air-sea interaction (Xue and Zhao, 2017). In El Niño developing summers, the warm pool convection is enhanced through a Gill-type response to positive SST anomalies in the central and eastern Pacific (Lau and Nath, 2000; Xue et al., 2018). In El Niño decaying summers, however, the warm pool convection is largely suppressed by eastward propagating Kelvin waves, which originate from the enhanced convection in the tropical Indian Ocean with a higher SST (Yang et al., 2007; Xie et al., 2009). The warm pool convection is, therefore, suggested as serving a bridge linking El Niño and the EASM.

The warm pool convection is also affected by the local SST anomaly, which is often involved with ENSO (Lau and Nath, 2009). Lu and Lu (2014) noted that a local SST plays an active role in the warm pool convection and partially offsets the remote effect from ENSO. Hu and Wu (2016) found that physical processes are very different for seasonal anomalies and the monthly departure from the seasonal mean over the South China Sea and tropical Indian Ocean during the spring-to-summer season. Although the remote forcing plays a major role in the seasonal anomaly, the local air-sea interaction is more pronounced in the monthly mean departure. We also note that

because El Niño in the decaying summers has a very strong impact on the warm pool convection, the influences of local air-sea interactions may be overwhelmed by the El Niño forcing in correlation or composite analyses.

In this study, we found that there is a significant correlation of convective activity in the warm pool between June and August while the correlations between other summer months are relatively weak. Because this correlation is independent of the phase of ENSO, it cannot be explained by the ENSO forcing. To address this issue, we conduct a detailed analysis based on the reanalysis data from 1979 to 2013. In Section 2, the monthly correlations of convective activity in the warm pool are briefly described. Some typical examples are further analyzed in Sections 3 and 4 to reveal the underlying physical processes and mechanisms. Finally, a summary is given in the last section.

2. Data description and monthly correlation of convective activity in the warm pool

Outgoing longwave radiation (OLR) data are used as a proxy for tropical convection, and are obtained from NOAA satellite observation (Liebmann and Smith, 1996). Other datasets include the atmospheric circulation and surface flux data from NCEP-DOE Reanalysis-2 (Kanamitsu et al., 2002), and SST data from NOAA (Smith et al., 2008). The horizontal resolutions of SST, atmospheric circulation (OLR) and surface flux are 2.0°×2.0°, 2.5°×2.5° and 1.904°×1.875° latitude/longitude, respectively. Since the OLR data are only available from 1979 to 2013, all datasets are analyzed during this 35-year period for consistency.

Considering the largest interannual variability of convection in the tropical western Pacific, Lu

(2001b) defined the warm pool convection as the mean OLR averaged over (110°-160°E, 10°-20°N), and a negative (positive) OLR anomaly corresponds to enhanced (suppressed) convection. Figure 1 shows the time series of the normalized OLR anomaly, in which the OLR anomaly series are compared between two different summer months in each subfigure. The correlation coefficients of monthly OLR anomalies between different summer months are remarkably different. The correlation coefficient of monthly OLR anomalies between June and July (r = 0.24) is statistically insignificant. By comparison, the correlation between June and August strengthens considerably (r = 0.52), which is substantially significant at the 99% confidence level. We also note that the correlation of OLR anomalies between July and August is very weak (r = -0.05) and insignificant, thus indicating the lack of linkage in warm pool convection from July to August. The significant positive correlation of convective activity over the warm pool between June and August despite the weak connections between other summer months is not yet well understood.

Figure 2 shows the spatial distributions of monthly OLR correlations in the western Pacific. The most significant correlation between June and July is located to the east of 150°E while the correlations outside of this region are relatively weak (Fig. 2a). The distributions of correlation coefficients between June and August (Fig. 2b) are to a large degree different from those in Figure 2a. Significant correlations are found from the South China Sea to the west of 140°E, which are connected to the significant correlations near the equator. The spatial pattern of correlations between July and August (Fig. 2c) is somewhat similar to that in Figure 2a, except in the oceanic region to the south of Japan. In general, the spatial distributions of monthly OLR correlations

136 further demonstrate that there is a significant correlation of convective activity over the warm pool
137 between June and August as illustrated in Figure 1. We also note that, different from the warm pool
138 region, significant correlations persist from June to August near the equator. This indicates that the
139 physical mechanisms for the correlation in the two regions are different.

140 Previous studies have shown that the warm pool convection is affected by both local air-sea
141 interaction and ENSO. While the former plays a major role in the monthly anomaly, the latter is
142 more important to the summer seasonal mean (Lu and Lu, 2014; Hu and Wu, 2016). In order to
143 distinguish the two factors governing the convection variability on different timescales more clearly,
144 band-pass (30-90 days) and low-pass (>90 days) filters are applied to daily OLR time series,
145 respectively. Figure 3 illustrates the spatial distributions of monthly OLR correlations between
146 summer months based on band-pass data. It is evident that the correlation patterns in the warm pool
147 region are quite different from those in Figure 2. The correlation between June and July (Fig. 3a) is
148 negative to the north of 10°N from the South China Sea to the date line, with three significant
149 centers located in the South China Sea, 135°E and 165°E. By comparison, a significantly positive
150 correlation is found near the equator. The correlation patterns between July and August are very
151 similar to those between June and July (Fig. 3c), except that the correlations to the east of the
152 Philippines are more significant. Both the negative correlations in the warm pool region and the
153 positive correlations near the equator between consecutive summer months (i.e., June and July in
154 Fig. 3a and, July and August in Fig. 3c) lead to the substantially significant positive correlations
155 over the entire western Pacific between June and August (Fig. 3b). The correlation coefficients are

above 0.8 near the equator and around 0.7 in the warm pool region. It should be noted that the positive correlation in the warm pool region between June and August is caused by the negative correlations between consecutive summer months, which can be attributed to the effect of local air-sea interactions.

Except for the positive correlations near the equator, the correlation distributions based on the low-pass data are dramatically different from the band-pass result (Fig. 4). The correlations between June and July (Fig. 4a) are somewhat similar to the original result in Figure 2a, but the correlations to the east of the Philippines are more significant, indicating that a weakly positive correlation of convective activity in the warm pool between June and July (r = 0.24, Fig. 1a) is mainly related to ENSO. In addition, the correlation in southern China is also more significant. Similar to the original result (Fig. 2c), the significant correlations between July and August are mainly located in the regions to the east of 150°E and to the east of Taiwan, but the correlations in the warm pool region are very weak (Fig. 4c). The correlations between June and August (Fig. 4b) are also weak in all other regions except for the equatorial region, which are quite different from those in Figure 2b and Figure 3b. This implies that the significant correlation of convective activity over the warm pool between June and August (r = 0.52, Fig. 1b) is not caused by ENSO.

A close examination of the OLR anomaly series in Figure 1b indicates that years with consistent negative OLR anomalies between June and August far exceed those with consistent positive OLR anomalies. Altogether, there are 8 years with significant negative anomalies below a -0.5 standard deviation, i.e., 1981, 1984, 1985, 1986, 1990, 2001, 2004 and 2012, and the anomaly

is below a -1 standard deviation in 1984, 1985 and 2004. By contrast, there are only 3 years with significant positive anomalies above a 0.5 standard deviation, i.e., 1980, 1996 and 1998, in which the anomaly is above a 1 standard deviation only in 1998. Although both the consistent positive and negative anomalies contribute to the positive correlation of OLR anomalies between June and August, the years with negative anomalies play a dominant role. We also note that the consistent positive OLR anomalies in 1980 and 1998 persist throughout the whole summer from June to August. This implies that the physical mechanism for the negative anomaly is different from that of the positive one. In addition, there is a maximum difference between June and August in 2007, with a positive anomaly in June and a negative anomaly in August. In the following sections, these years will be analyzed in detail to reveal the physical mechanism causing the significant correlation between June and August.

3. Intraseasonal variation of the warm pool convection in 1984 and 2004

As stated in the previous section, the strongest warm pool convection in June and August occurred in three years (i.e., 1984, 1985 and 2004). Since 1985 is similar to 1984 except for a slightly stronger La Niña signal, 1984 and 2004 are selected as the typical examples for an intercomparison. As shown in Figure 5, 1984 is a La Niña year, and 2004 is an El Niño developing year. As the absolute value of the monthly Niño3.4 Index is less than 1˚C from winter to summer during these two years, we may infer that the warm pool convection is not heavily influenced by the ENSO forcing. The SST anomalies in the spring seasons of 1984 and 2004 share a common feature

of a higher SST to the east of the Philippines (Fig. 6), thus indicating that the warm pool SST anomaly is not entirely dependent on the ENSO phase. Nonetheless, there are still some differences in the spring SST anomaly between these two years at a regional scale. While positive SST anomalies extend all over the western Pacific in 2004, negative SST anomalies appear over the East China Sea and the equatorial central Pacific in 1984 due to the La Niña forcing.

A higher SST in the preceding spring provides a favorable thermal condition for the convection's development in June. Figs. 7a and 7b illustrate that negative OLR anomalies (enhanced convection) over the warm pool in June of 1984 and 2004, respectively, coincide with positive SST anomalies in the preceding spring (Fig. 6). Moreover, due to a higher warm pool SST in the spring of 2004 than that in the spring of 1984, the OLR anomalies in June 2004 extend farther eastward with a minimum lower than -40 Wm^{-2}. Therefore, a positive SST anomaly in the preceding spring plays a major role in triggering the convection development in the following June.

The enhanced warm pool convection and the associated more cloud cover lead to decreased solar radiation at the surface. In June of 1984 and 2004 (Figs. 8a and 8b), significant negative downward solar radiation flux anomalies are found from the South China Sea to the east of the Philippines. The solar radiation flux anomaly patterns evidently resemble OLR anomaly patterns, thus confirming the essential role of the cloud-radiation effect in the monthly SST change. A reduced solar radiation results in a decreased local SST (Lu and Lu, 2014; Hu and Wu, 2016). As shown in Figure 9, negative SST anomalies from the South China Sea to 150°E are approximately -0.2˚C, with regional anomalies reaching -0.4˚C to -0.6˚C. We note that the SST anomaly value in

the South China Sea exceeds that to the east of the Philippines because deep convection in June is mainly located in the South China Sea and the convection to the east of the Philippines is not fully developed. By comparison, the SST anomalies over regions to the east of Taiwan and to the east of 150°E are opposite in these two years, which resembles their counterparts in spring (Fig. 6). This implies that the SST anomalies outside of the warm pool are possibly influenced by the ENSO signal and are less related to the local convection development.

Corresponding to negative SST anomalies in June, the warm pool convection in July is suppressed with positive OLR anomalies in both years, except that the OLR anomaly center in 1984 is located more southward than that in 2004 (Figs. 7c and 7d). Contrary to June convection, the suppressed convection in July is associated with less cloud cover, which further induces an increased solar radiation at the surface. As shown in Figs. 8c and 8d, the solar radiation tends to intensify in July over the warm pool region. Consequently, SST to the east of the Philippines tends to rise apparently with an amplitude of 0.5˚C from June to July (Figs. 10a and 10b). Over the South China Sea in 1984, a decrease in SST is still evident due to excessive convection development in June (Fig. 7a). We note that a prominent increase in SST to the north of 20°N results from the annual cycle from June to July and is entirely unrelated to the warm pool convection. Because there is a lower SST in June 1984 and a higher SST in June 2004 (Fig. 9), the former undergoes a more evident increase in SST than the latter (Figs. 10a and 10b).

In response to an SST increase in the warm pool, the warm pool convection is enhanced again with negative OLR anomalies in August (Figs. 7e and 7f). Like June, the major negative OLR

anomalies in August 1984 are located from the South China Sea to 140°E (Fig. 7e). In August 2004, the negative OLR anomalies extend southeastward to the equator. We stress that the OLR anomaly pattern near the equator in August 2004 resembles that in an El Niño developing August, which is related to the SST anomaly in the central Pacific due to the El Niño development (Xue et al., 2018). Similar to the case in June, the enhanced convection in August leads to a decrease of the solar radiation at the surface, especially from the South China Sea to the east of the Philippines (Figs. 8e and 8f), thus inducing a decrease in SST in August once more (Figs. 10c and 10d). While the major negative SST difference is located to the east of Taiwan in 1984 with a minimum of -1.0˚C, it is generally confined to the west of 150°E in 2004. Like the change from June to July, the SST difference is not exactly in agreement with the negative OLR anomaly center.

In summary, a significant correlation of convective activity over the warm pool between June and August mainly results from local air-sea interaction. When the warm pool SST is higher in spring, convection in June tends to enhance together with a decrease in SST. In turn, convection in July is suppressed due to a decreased SST. Conversely, the suppressed convection in July leads to an increase in SST. Accordingly, convection in August is enhanced once again. During this process, the warm pool convection in June is positively correlated with that in August. We emphasize that this phenomenon is only evident in the warm pool extending from the South China Sea to 150°E, where a deep convective system is observed in summer. In the equatorial zone to the east of 150°E, however, OLR maintains a positive anomaly from June to August due to a lower SST associated with the 1984 La Niña event (Fig. 7, left panel). This consistent anomaly is clearly reflected in the

monthly OLR correlation (Fig. 2), which is in accordance with previous results (Xue and Zhao, 2017).

Contrary to positive SST anomalies in spring, there are negative SST anomalies in summer over the warm pool due to enhanced convection especially in June and August (Fig. 11). Since convection develops earliest in the South China Sea, a lower SST is evident there in 1984 and 2004. Like the SST anomaly in June (Fig. 9), the SST anomalies to the east of 150°E near the equator are almost opposite between the two years. In addition to local air-sea interactions, the SST anomalies in the tropical western Pacific, especially outside of the warm pool, are also affected by the La Niña in 1984 and El Niño in 2004.

The enhanced convection is associated with more precipitation in the warm pool. Lu and Lu (2014) classified the summers of 1984 and 2004 over the warm pool into a climate type characterized by a negative SST anomaly and a positive precipitation anomaly and attributed this SST-precipitation relationship to the atmospheric forcing. However, our analysis results suggest that convection development in June actually originates from a higher SST in the preceding spring while the atmospheric forcing plays a major role in the intraseasonal shift of the OLR anomaly from June to July. Therefore, not only the concurrent summer SST anomaly but also the preceding spring SST anomaly must be taken into consideration to fully interpret the warm pool convection anomaly.

4. Competing effects on the warm pool convection in 1998 and 2007

In addition to the consistent negative OLR anomalies in June and August discussed previously,

there are consistent positive OLR anomalies (suppressed warm pool convection) in some years. The most significant positive anomalies are found in 1998, when the OLR anomalies in June and August exceed a 1 standard deviation (Fig. 1b). The OLR difference between June and August reaches a maximum in 2007 during the 1979-2013 period, with a positive anomaly in June and a negative one in August. To further understand the significant correlation of convective activity in the warm pool between June and August from a different viewpoint, we select 1998 and 2007 for a comparison with the result in Section 3.

The Niño3.4 Index indicates that both 1998 and 2007 are El Niño decaying years, except that the El Niño intensity in 1998 is much stronger than that in 2007 (Fig. 12). The maximum of the monthly Niño3.4 Index during the 1997-1998 El Niño event exceeds 2.0˚C while the maximum during the 2006-2007 event is approximately 1.0˚C. Furthermore, the El Niño event in 1998 decays more rapidly and changes into a La Niña state in summer. The Niño3.4 Index in August 1998 is below -1.0˚C, whereas it is around -0.5˚C in summer of 2007. Due to the influence from El Niño, there is a consistent higher SST over the Indian Ocean from the El Niño mature winter to the decaying summer. During the decaying spring, positive SST anomalies are evident in the tropical Indian Ocean, and the anomaly in 1998 is more prominent than that in 2007 due to the difference in El Niño intensity (Fig. 13). Some discrepancies are found at a regional scale. While positive and negative SST anomalies are seen in the Bay of Bengal and to the east of the Philippines, respectively, in spring of 1998, the opposite SST anomalies appear over these regions in spring of 2007.

296 Previous studies showed that, during an El Niño decaying summer, the warm pool convection
297 is suppressed by Kelvin waves propagating eastward from enhanced convection in the tropical
298 Indian Ocean (Xie et al., 2009; Wu et al., 2010). As illustrated in Figure 14, the warm pool OLR
299 maintains positive anomalies in June and July for both years. In August, OLR in 2007 shifts to a
300 negative anomaly, while a positive anomaly persists in 1998.

301 The difference in the warm pool OLR anomaly in August between 1998 and 2007 can be
302 attributed to the competing effects of El Niño forcing and local air-sea interactions. Because the El
303 Niño intensity in 2007 is much weaker than that in 1998, the convection anomaly over the Indian
304 Ocean in August 2007 is weaker than that in August 1998 (Figs. 14e and 14f). Furthermore, the
305 warm pool SST tends to rise with the suppressed convection from June to July. The monthly
306 difference in SST indicates an increase in SST to the east of the Philippines from June to July, with
307 a larger increase in 1998 (Figs. 15a and 15b). With an SST increase in July and a weaker forcing
308 from the Indian Ocean in August 2007, the warm pool OLR shifts to a negative anomaly due to
309 local air-sea interaction (Fig. 14f). Accordingly, the warm pool SST decreases from July to August
310 (Fig. 15d). This process is similar to those in 1984 and 2004 as shown in Section 3. By contrast, the
311 warm pool SST continues to rise from July to August because of a stronger forcing from the Indian
312 Ocean in 1998 (Fig. 15c).

313 A comparison between these two years implies that there is a complex relationship between El
314 Niño and the June-August correlation of convective activity in the warm pool. When an El Niño is
315 very strong like 1998, the consistent positive OLR anomalies persist from June to August, and the

El Niño forcing plays a positive role in the significant correlation between June and August. When an El Niño is not strong like 2007, the effect of local air-sea interactions dominates over the El Niño forcing to determine the convection anomaly in the late summer. The aforementioned results indicate that the effect of local air-sea interactions on the warm pool convection is only evident when the El Niño signal is not strong. Likewise, in strong La Niña years, as in 1989 and 1999, there is not a consistent anomaly of the warm pool convection between June and August (Fig. 1b). In this case, the warm pool convection is directly dominated by La Niña forcing although the warm pool SST is higher in the preceding spring (Xue and Zhao, 2017).

5. Summary

Based on the monthly OLR data from 1979 to 2013, we found a significant positive correlation of convective activity over the warm pool between June and August. Years with consistent negative OLR anomalies (i.e., the enhanced warm pool convection) in June and August play a dominant role in this correlation. Two prerequisites are essential for this significant correlation, i.e., a higher SST in the preceding spring over the warm pool and a relatively weak ENSO signal. The former provides a thermal condition for the convection development in June, while the latter ensures that the warm pool convection is less affected by ENSO. A correlation analysis based on band-pass and low-pass filtered data further demonstrates that ENSO is not a major factor in this June-August correlation.

We select 1984 and 2004 as typical examples to further investigate the physical mechanisms

for the consistent and significant negative OLR anomalies in June and August. In 1984 and 2004, a higher SST in the preceding spring over the warm pool leads to enhanced convection in the following June, which further induces decreased downward shortwave radiation at the surface and decreased local SST. As a result, convection in July is suppressed and the solar radiation at the surface tends to rise again together with local SST. Similar to the June convection, the convection in August tends to enhance once more. During this process, a consistent anomaly appears over the warm pool in June and August. Clearly, local air-sea interaction plays a dominant role in the June-August correlation.

In addition to 1984 and 2004, there are some other years in Figure 1 showing consistent negative OLR anomalies below a -0.5 standard deviation in June and August (i.e., 1981, 1985, 1986, 1990, 2001 and 2012). Figure 16 further shows the composite OLR anomaly for these years. In general, the composite result shares a common feature with the individual years of 1984 and 2004 in Figure 7. Negative OLR anomalies appear in June and August and are interrupted by a positive one in July from the South China Sea to the east of the Philippines. However, the significance in July is statistically lower than that in June and August. Combined with the results in 1984 and 2004, we are more confident that the local effect is a major driver in the June-August correlation. By contrast, the anomaly between June and August is not consistent in strong La Niña years although the warm pool is abnormally warmer in spring. In this case, the warm pool convection is enhanced throughout the whole summer with a strongest anomaly in July (Xue and Zhao, 2017). Interestingly, the correlation is only evident in the warm pool where deep convective systems are observed. In the

equatorial region, however, the OLR anomaly is mainly affected by ENSO instead of the local effect.

There is a complex relationship between the June-August convection correlation and El Niño. When an El Niño signal is very strong (e.g., 1998), the consistent positive OLR anomalies induced by the El Niño forcing throughout the whole summer contribute to the positive convection correlation. When the signal is not so strong (e.g., 2007), positive OLR anomalies during June and July can be attributed to the El Niño forcing. After the forcing weakens in August, OLR shifts to a negative anomaly due to local air-sea interactions. The combined effects of local and remote factors result in opposite OLR anomalies between June and August. Despite the positive role of strong El Niño forcing on the correlation, the local effect is the principal reason for the significant positive correlation of convective activity in the warm pool between June and August.

Previous studies have suggested that, as the strongest signal in the tropics, ENSO plays a crucial role in the warm pool convection and the EASM. ENSO is also used as a major indicator for the EASM prediction (Xue et al., 2015). When the ENSO signal is not strong as in 1984 and 2004, the warm pool convection may be enhanced due to local air-sea interaction from a higher SST in the preceding spring. In this case, the WPSH tends to retreat eastward with less rainfall in eastern China. Additionally, the result provides a reliable signal for the EASM prediction. When the ENSO signal is not strong, the warm pool SST anomaly in spring and the related local air-sea interactions should be paid more attention, so the EASM prediction can be improved (Duan et al., 2008; Lau and Nath, 2009).

The results presented in this study show an approximate feature of the warm pool convection associated with local air-sea interactions based on monthly mean data. It is apparent that we must delineate the interactions between the warm pool convection and SST in more detail by using daily data. Moreover, a numeral simulation using an air-sea coupled model is also essential to further reveal the physical mechanism causing this correlation.

Acknowledgements. The authors appreciate the comments and suggestions from the two anonymous reviewers and the editor Dr. Hiroaki Miura. This study is supported by the National Science Foundation of China (Grant No. 41475052 and 41630530).

REFERENCES

Ding, Y. H., and Y. Liu, 2001: Onset and the evolution of the summer monsoon over the South China Sea during SCSMEX field experiment in 1998. *J. Meteor. Soc. Japan*, **79**(1B), 255-276.

Duan, A., C. Sui, and G. Wu, 2008: Simulation of local air-sea interaction in the great warm pool and its influence on Asian monsoon. *J. Geophy. Res.*, **113**(D22), https://doi.org/10.1029/2008JD010520

Hu, W.-T., and R. Wu, 2016: Air-sea interaction in association with monthly anomaly departure over the South China Sea and tropical Indian Ocean during the spring-to-summer transition. *J. Climate*, **29**, 2095–2108.

Kanamitsu, M., W. Ebisuzaki, J. Woollen, S.-K. Yang, J. J. Hnilo, M. Fiorino, and G. L. Potter, 2002: NCEP-DOE AMIP-II Reanalysis (R-2). *Bull. Amer. Meteor. Soc.*, **83**, 1631–1643.

Lau, K.-M., and S. Yang, 1997: Climatology and interannual variability of the southeast Asian summer monsoon. *Adv. Atmos. Sci.*, **14**, 141–162.

Lau, N.-C., and M. J. Nath, 2000: Impact of ENSO on the variability of the Asian–Australian monsoons as simulated in GCM experiments. *J. Climate*, **13,** 4287–4309.

Lau, N.-C., and M. J. Nath, 2009: A model investigation of the role of air–sea interaction in the climatological

401 evolution and ENSO-related variability of the summer monsoon over the South China Sea and western North
402 Pacific. *J. Climate*, 22, 4771–4792.
403 Liebmann, B., and C. A. Smith, 1996: Description of a complete (interpolated) outgoing longwave radiation
404 dataset. *Bull. Amer. Meteor. Soc.*, **77**, 1275–1277.
405 Lu, R., 2001a: Interannual variability of the summertime North Pacific subtropical high and its relation to
406 atmospheric convection over the warm pool. *J. Meteor. Soc. Japan*, **79**, 771–783.
407 Lu, R., 2001b: Atmospheric circulations and sea surface temperatures related to the convection over the western
408 Pacific warm pool on the interannual scale. *Adv. Atmos. Sci.*, **18**, 270–282.
409 Lu, R., and S. Lu, 2014: Local and remote factors affecting the SST–precipitation relationship over the western
410 North Pacific during summer. *J. Climate*, **27**, 5132–5147.
411 Nitta, T., 1987: Convective activities in the tropical western Pacific and their impact on the northern hemisphere
412 summer circulation. *J. Meteor. Soc. Japan*, **65**, 373–390.
413 Smith, T. M., R. W. Reynolds, T. C. Peterson, and J. Lawrimore, 2008: Improvements to NOAA's historical
414 merged land–ocean surface temperature analysis (1880–2006). *J. Climate*, **21**, 2283–2296.
415 Su, T. H., and F. Xue, 2010: The intraseasonal variation of summer monsoon circulation and rainfall in East Asia.
416 *Chinese J. Atmos. Sci.*, **34**(3), 611–628. (in Chinese)
417 Tao, S. Y., and L. X. Chen, 1987: A review of recent research on the East Asian summer monsoon in China.
418 *Monsoon Meteorology*, C.-P. Chang and T. N. krishnamurti, Eds., Oxford University Press, 60–92.
419 Tsuyuki, T., and K. Kurihara, 1989: Impact of convective activity in the western tropical Pacific on the East Asian
420 summer circulation. *J. Meteor. Soc. Japan*, **67**, 231–247.
421 Ueda, H., and T. Yasunari, and R. Kawamura, 1995: Abrupt seasonal change of large-scale convective activity
422 over the western Pacific in the northern summer. *J. Meteor. Soc. Japan*, **73**, 795–809.
423 Wu, R., 2002: Processes for the northeastward advance of the summer monsoon over the western north Pacific. *J.*
424 *Meteor. Soc. Japan*, **80**, 67–83.
425 Wu, B., T. Li, and T. Zhou, 2010: Relative contributions of the Indian Ocean and local SST anomalies to the
426 maintenance of the western North Pacific anomalous anticyclone during the El Niño decaying summer. *J.*
427 *Climate*, **23**, 2974–2986.

Xie, S.-P., K. Hu, J. Hafner, H. Tokinaga, Y. Du, G. Huang, and T. Sampe, 2009: Indian Ocean capacitor effect on Indo–western Pacific climate during the summer following El Niño. *J. Climate*, **22**, 730–747.

Xue, F., Q. C. Zeng, R. H. Huang, C. Y. Li, R. Y. Lu, and T. J. Zhou, 2015: Recent advances in monsoon studies in China. *Adv. Atmos. Sci.*, **32**, 206–229.

Xue, F., and J. J. Zhao, 2017: Intraseasonal variation of the East Asian summer monsoon in La Niña years. *Atmos. Oceanic Sci. Lett.*, **10**,156–161.

Xue, F., X. Dong, and F. Fan, 2018: Anomalous western Pacific subtropical high in El Niño developing summer and its comparison with the decaying summer. *Adv. Atmos. Sci.*, **35**, 360–367.

Yang, J., Q. Liu, S.-P. Xie, Z. Liu, and L. Wu, 2007: Impact of the Indian Ocean SST basin mode on the Asian summer monsoon. *Geophys. Res. Lett.*, **34**, L02708, doi:10.1029/2006GL028571.

List of Figures

anomalies over the warm pool below -0.5 standard deviation (i.e., 1981, 1984, 1985, 1986, 1990, 2001, 2004, and 2012), (a) June, (b) July, (c) August, regions above the 95% confidence level are shaded.

Fig.1

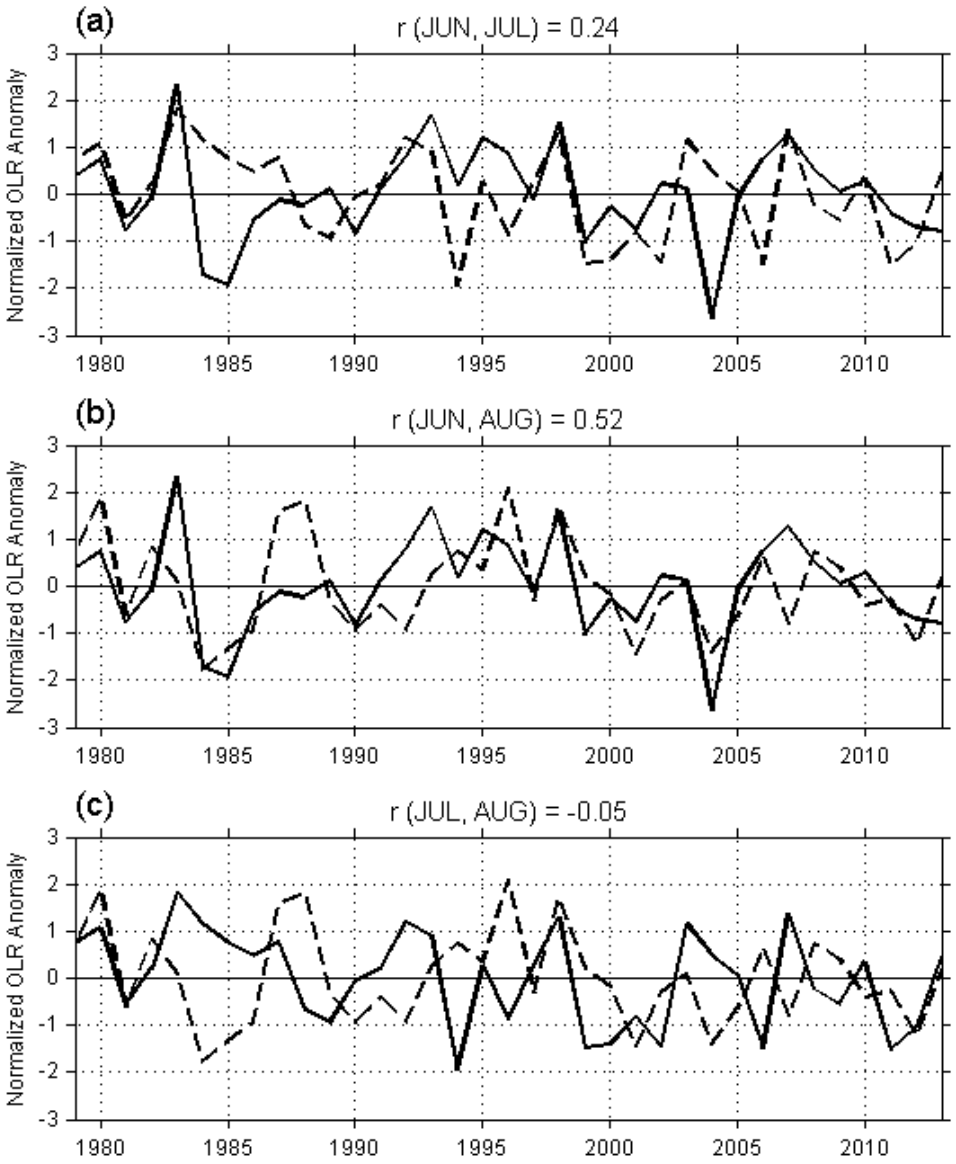
(a)
r (JUN, JUL) = 0.24
(b)
r (JUN, AUG) = 0.52
(c)
r (JUL, AUG) = -0.05
Normalized OLR Anomaly
3
2
1
0
-1
-2
-3
1980
1985
1990
1995
2000
2005
2010

Fig. 2

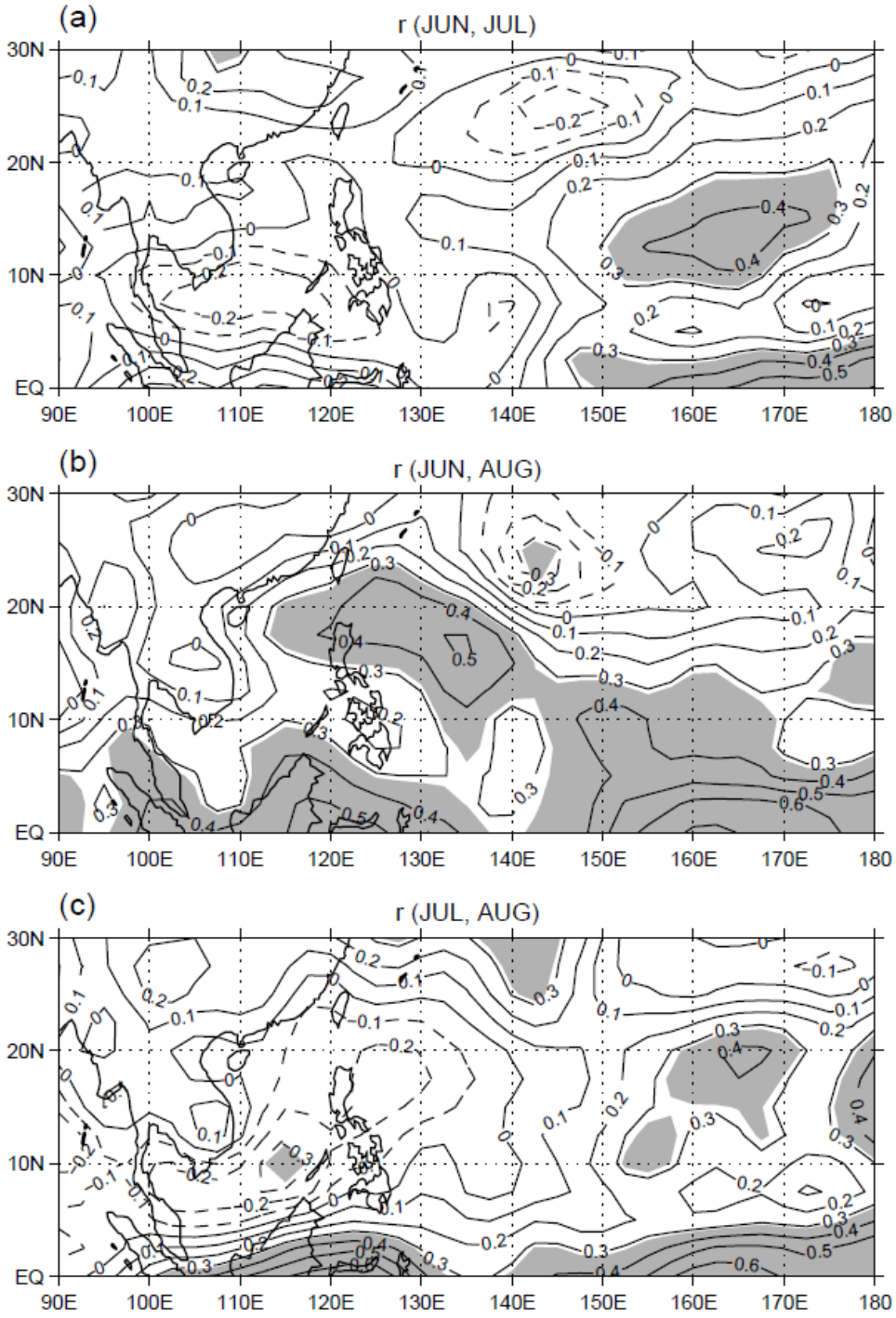
(a)
r (JUN, JUL)
(b)
r (JUN, AUG)
(c)
r (JUL, AUG)
30N
20N
10N
EQ
90E
100E
110E
120E
130E
140E
150E
160E
170E
180

499

500 Fig. 3

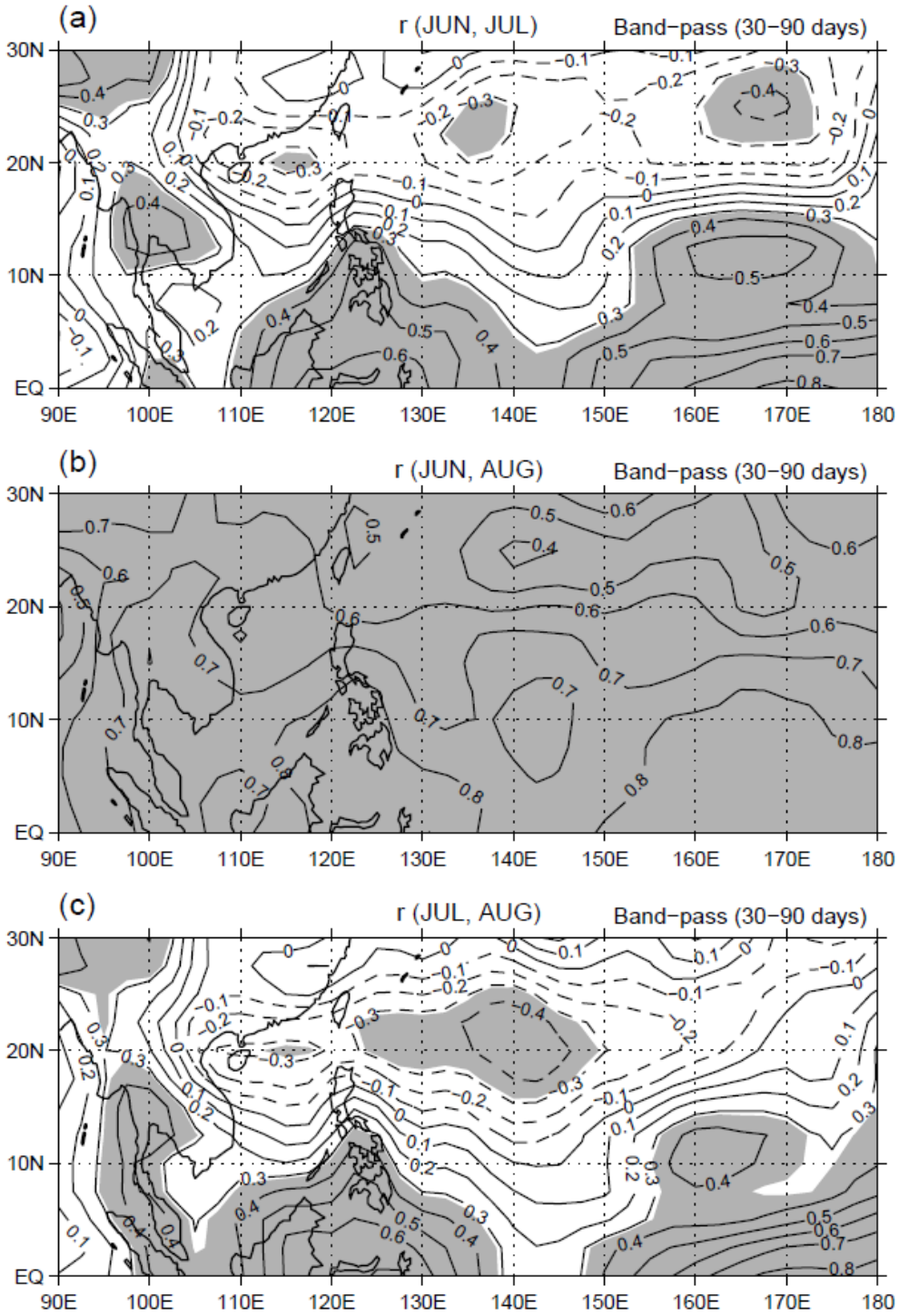

501

502

503

504

505 Fig. 4

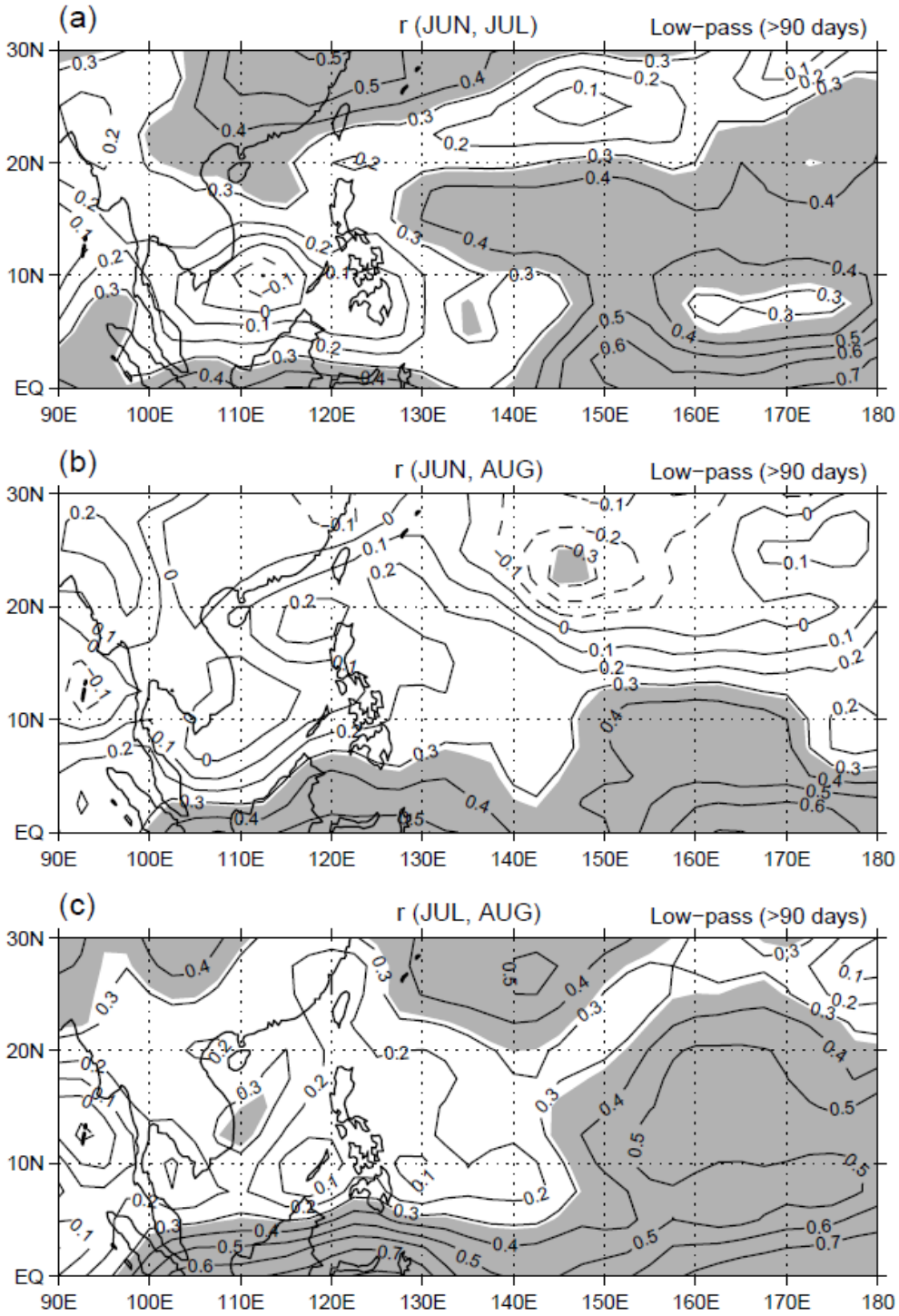

506

507

508

Fig. 5

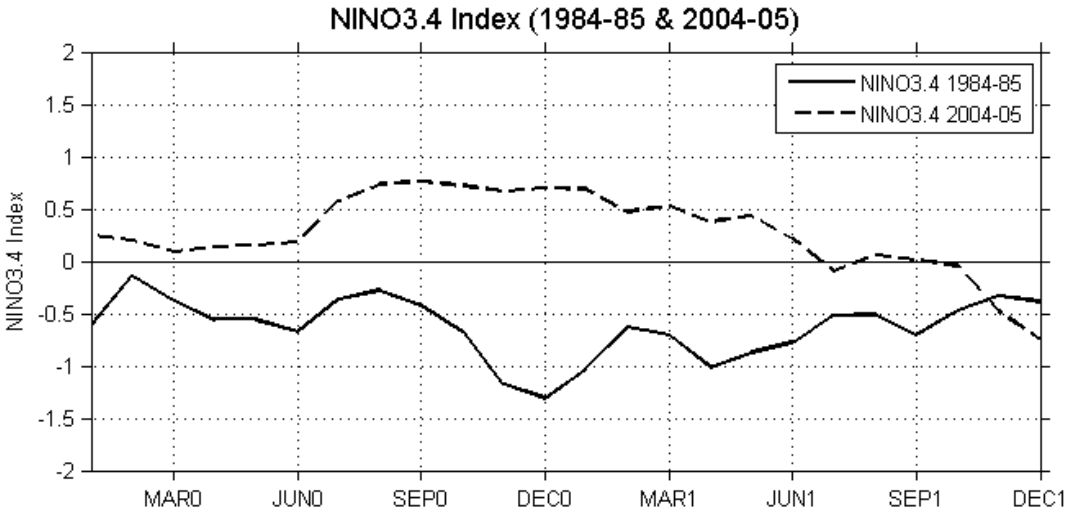
NINO3.4 Index (1984-85 & 2004-05)
NINO3.4 1984-85
NINO3.4 2004-05
NINO3.4 Index
2
1.5
1
0.5
0
-0.5
-1
-1.5
-2
MAR0
JUN0
SEP0
DEC0
MAR1
JUN1
SEP1
DEC1

Fig. 6

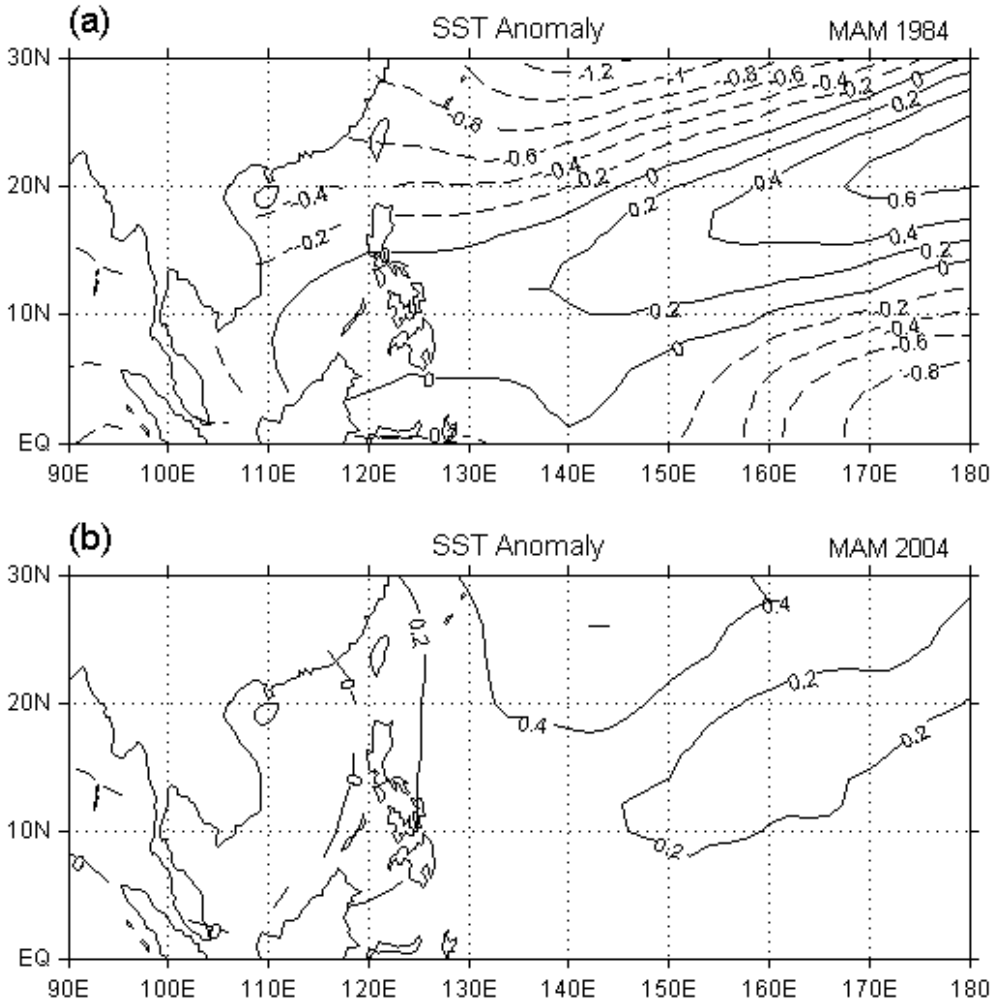
(a)
SST Anomaly
MAM 1984
30N
20N
10N
EQ
90E
100E
110E
120E
130E
140E
150E
160E
170E
180
(b)
SST Anomaly
MAM 2004
30N
20N
10N
EQ
90E
100E
110E
120E
130E
140E
150E
160E
170E
180

Fig. 7

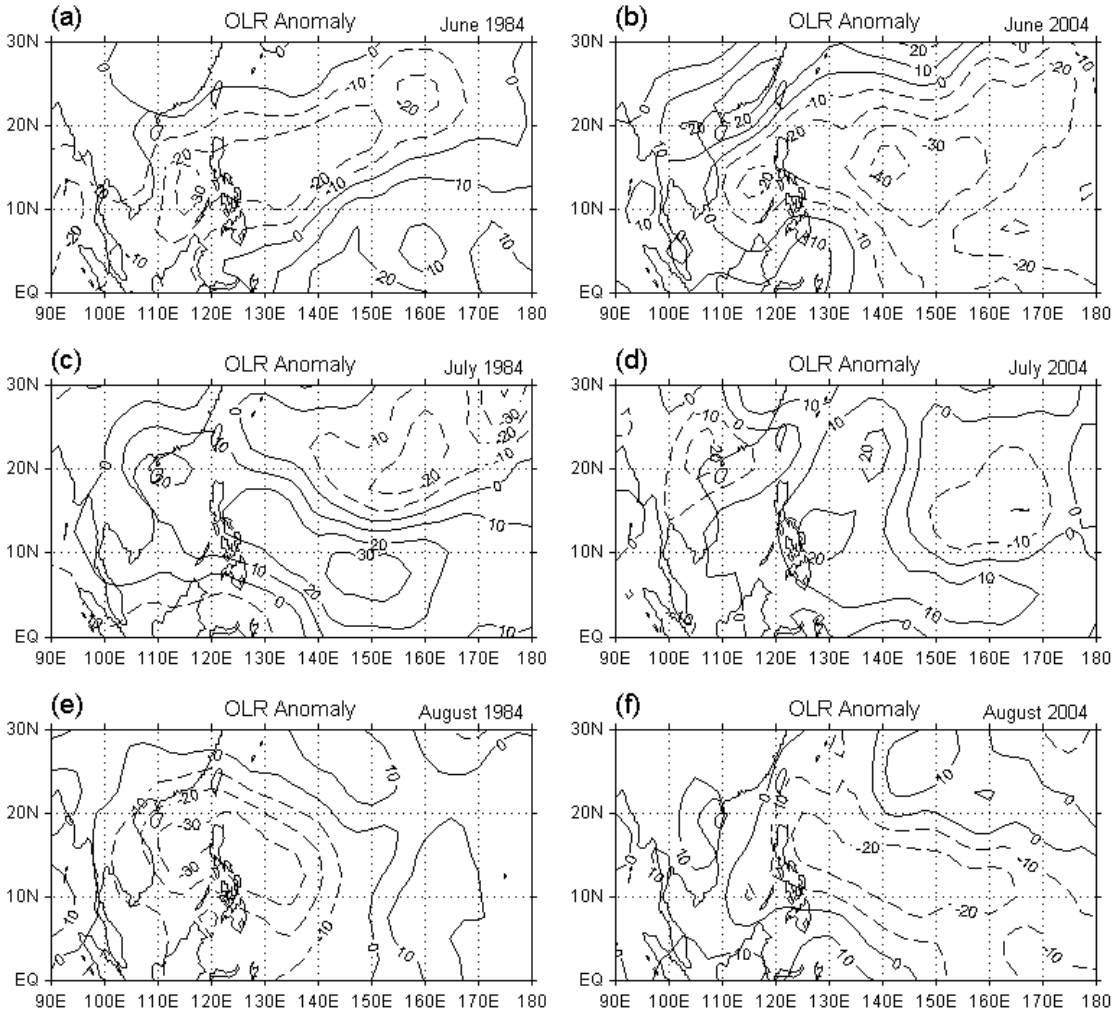
(a) OLR Anomaly June 1984
(b) OLR Anomaly June 2004
(c) OLR Anomaly July 1984
(d) OLR Anomaly July 2004
(e) OLR Anomaly August 1984
(f) OLR Anomaly August 2004
30N
20N
10N
EQ
90E 100E 110E 120E 130E 140E 150E 160E 170E 180

Fig. 8

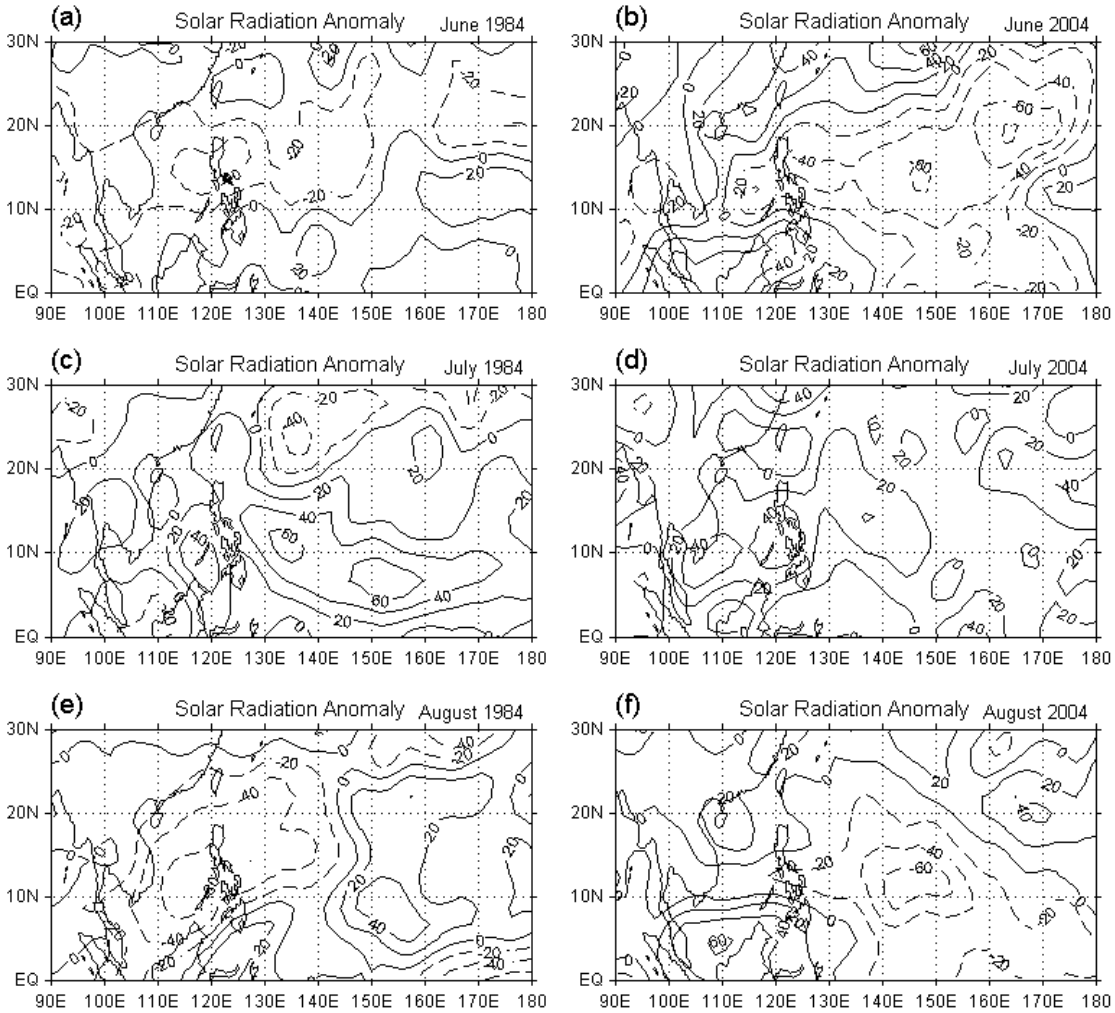
(a) Solar Radiation Anomaly June 1984
(b) Solar Radiation Anomaly June 2004
(c) Solar Radiation Anomaly July 1984
(d) Solar Radiation Anomaly July 2004
(e) Solar Radiation Anomaly August 1984
(f) Solar Radiation Anomaly August 2004
30N
20N
10N
EQ
90E 100E 110E 120E 130E 140E 150E 160E 170E 180

Fig. 9

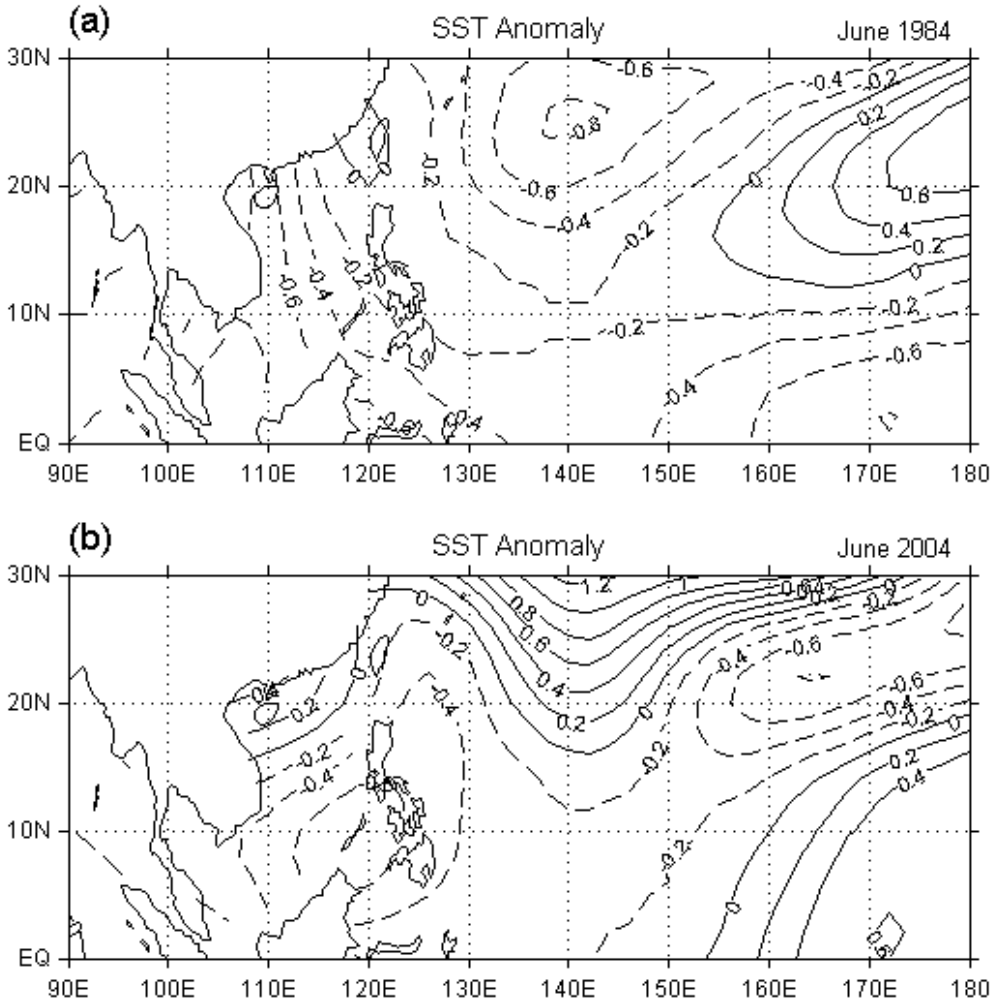
(a)
SST Anomaly
June 1984
30N
20N
10N
EQ
90E
100E
110E
120E
130E
140E
150E
160E
170E
180
(b)
SST Anomaly
June 2004
30N
20N
10N
EQ
90E
100E
110E
120E
130E
140E
150E
160E
170E
180

Fig. 10

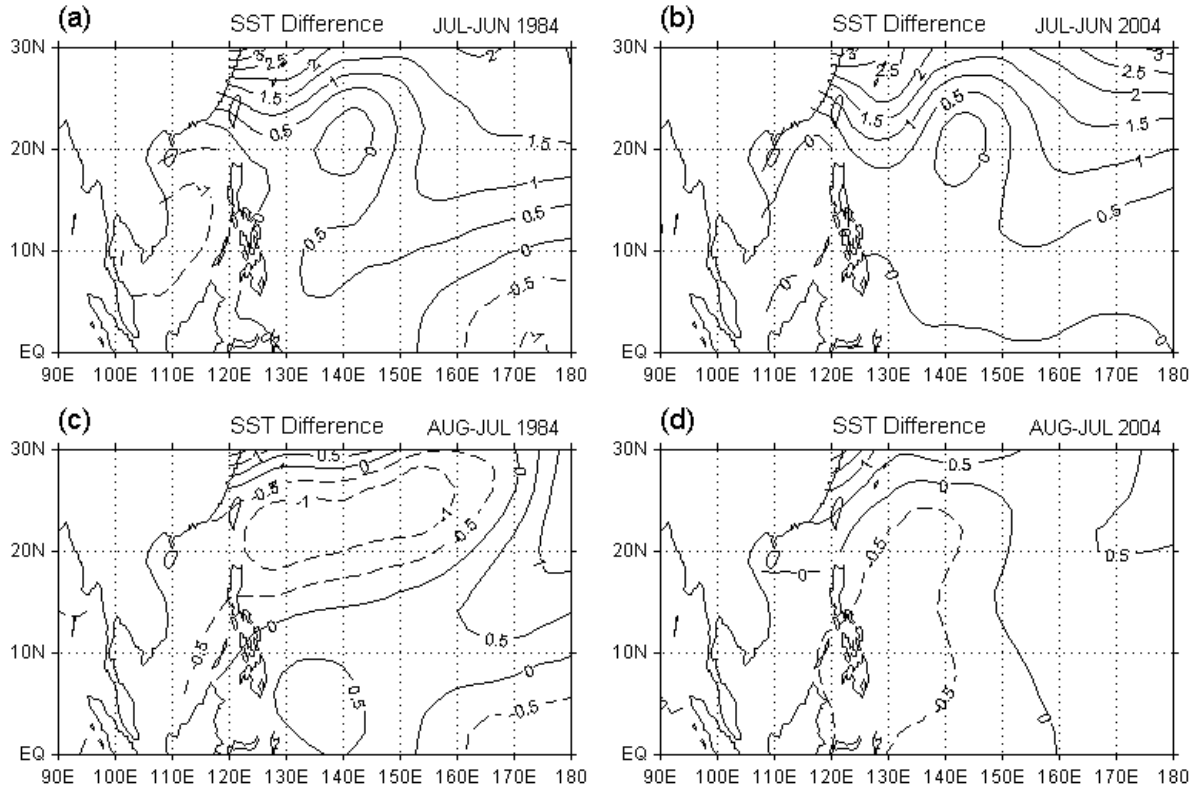
(a)
SST Difference
JUL-JUN 1984
(b)
SST Difference
JUL-JUN 2004
(c)
SST Difference
AUG-JUL 1984
(d)
SST Difference
AUG-JUL 2004
30N
20N
10N
EQ
90E 100E 110E 120E 130E 140E 150E 160E 170E 180

Fig. 11

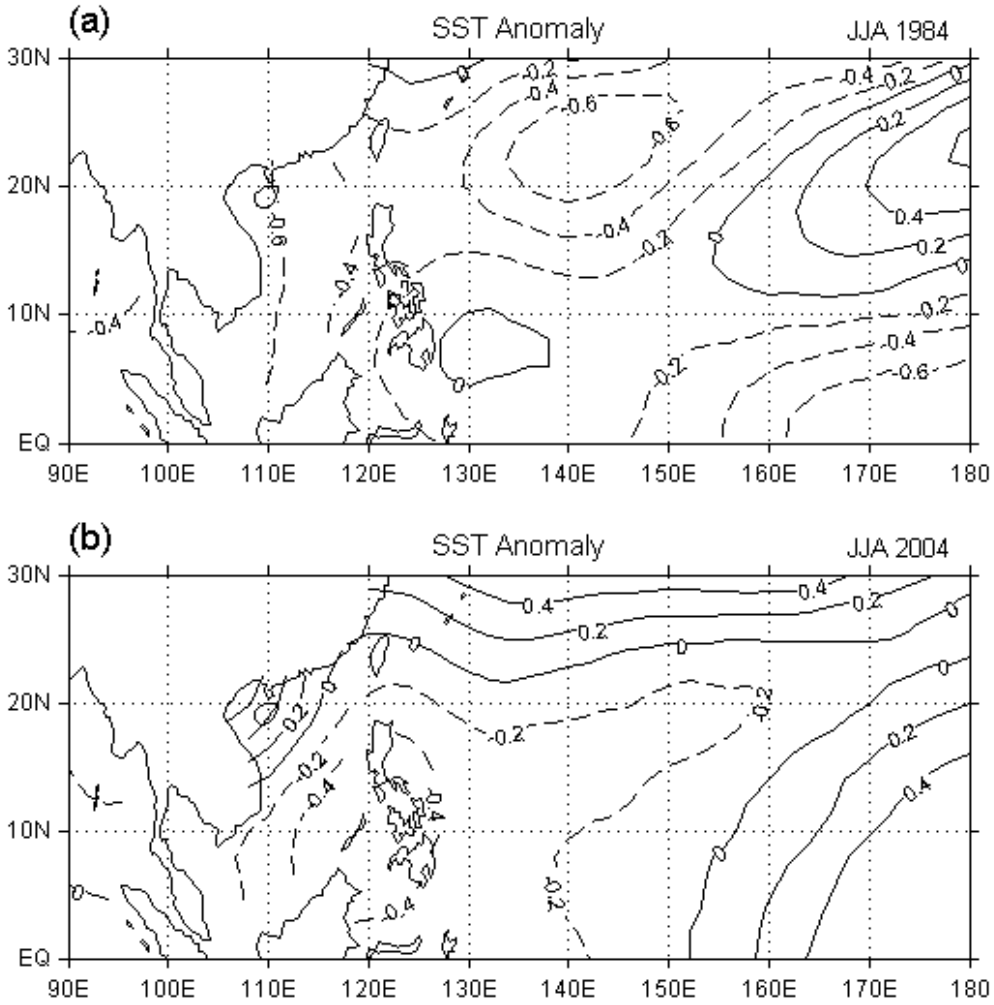
(a)
SST Anomaly
JJA 1984
30N
20N
10N
EQ
90E
100E
110E
120E
130E
140E
150E
160E
170E
180
(b)
SST Anomaly
JJA 2004
30N
20N
10N
EQ
90E
100E
110E
120E
130E
140E
150E
160E
170E
180

608

609 Fig. 12

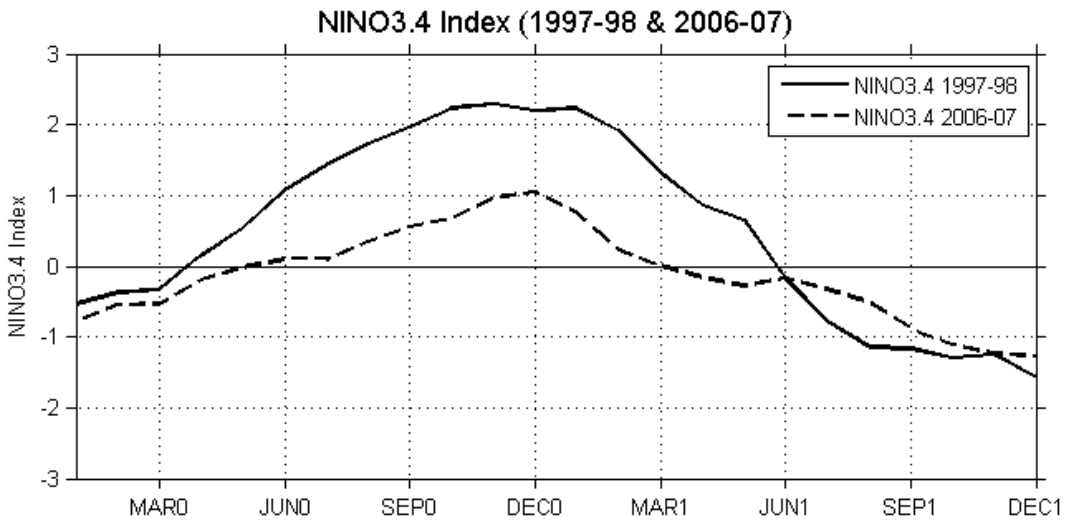

610

611

612

613

614

615

616

617

618

619

620

621

622

623

624

625

626

627

628 Fig. 13

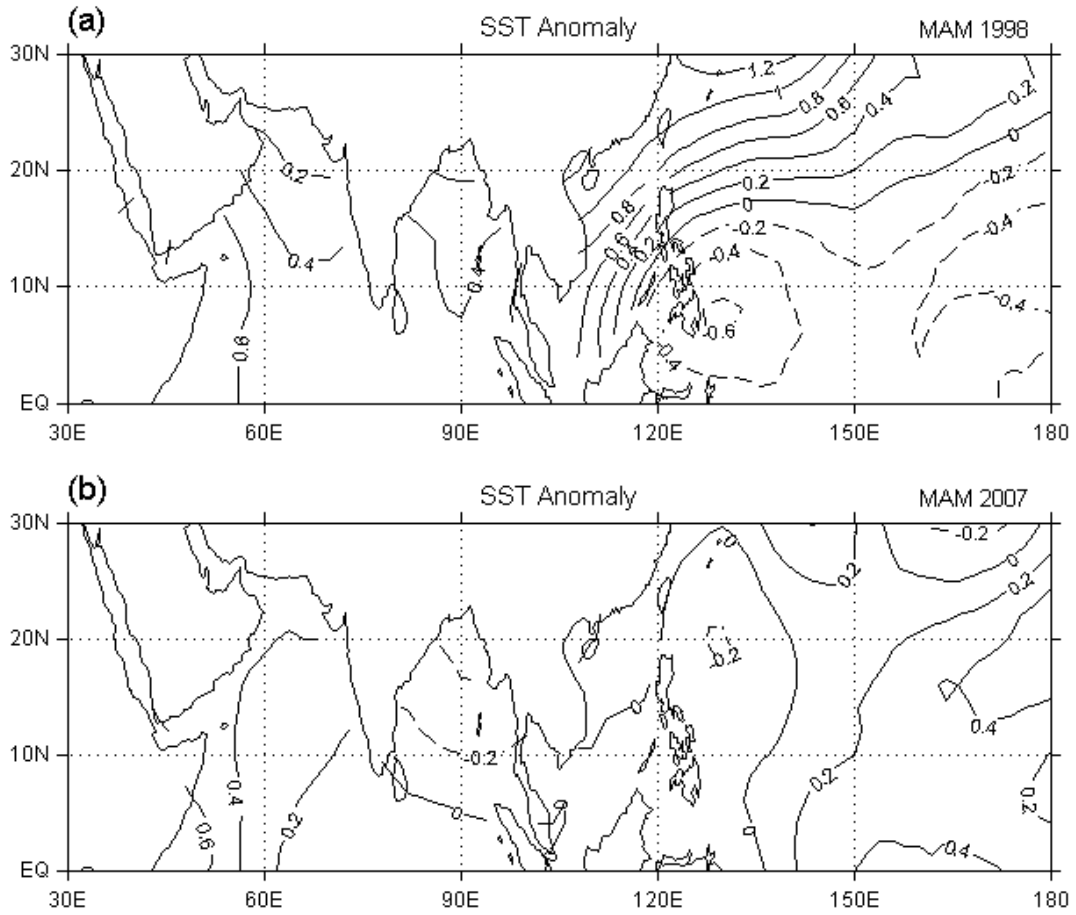

629

630

631

632

633

634

635

636

637

638

639

640

Fig. 14

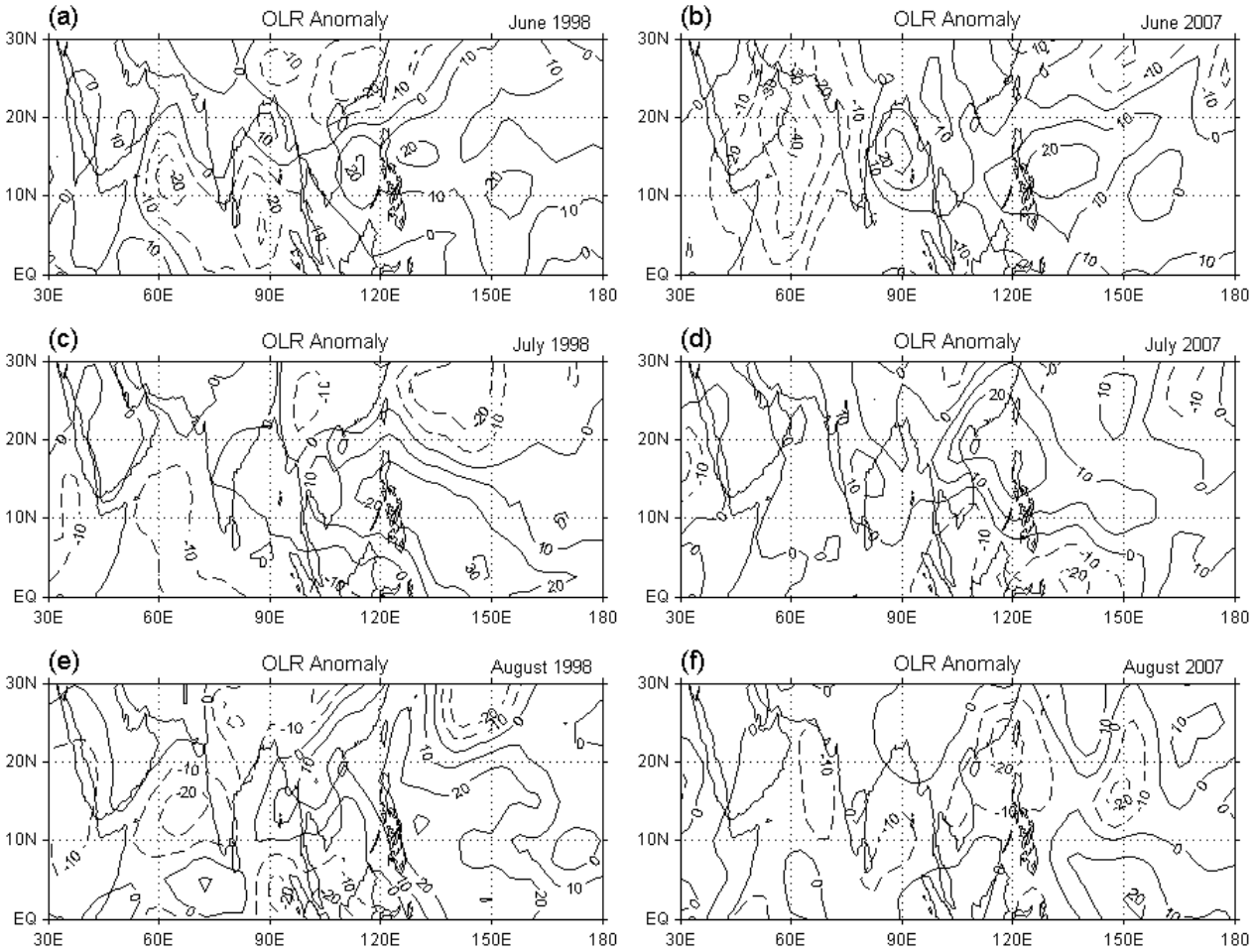
(a)
OLR Anomaly
June 1998
(b)
OLR Anomaly
June 2007
(c)
OLR Anomaly
July 1998
(d)
OLR Anomaly
July 2007
(e)
OLR Anomaly
August 1998
(f)
OLR Anomaly
August 2007
30N
20N
10N
EQ
30E
60E
90E
120E
150E
180

Fig. 15

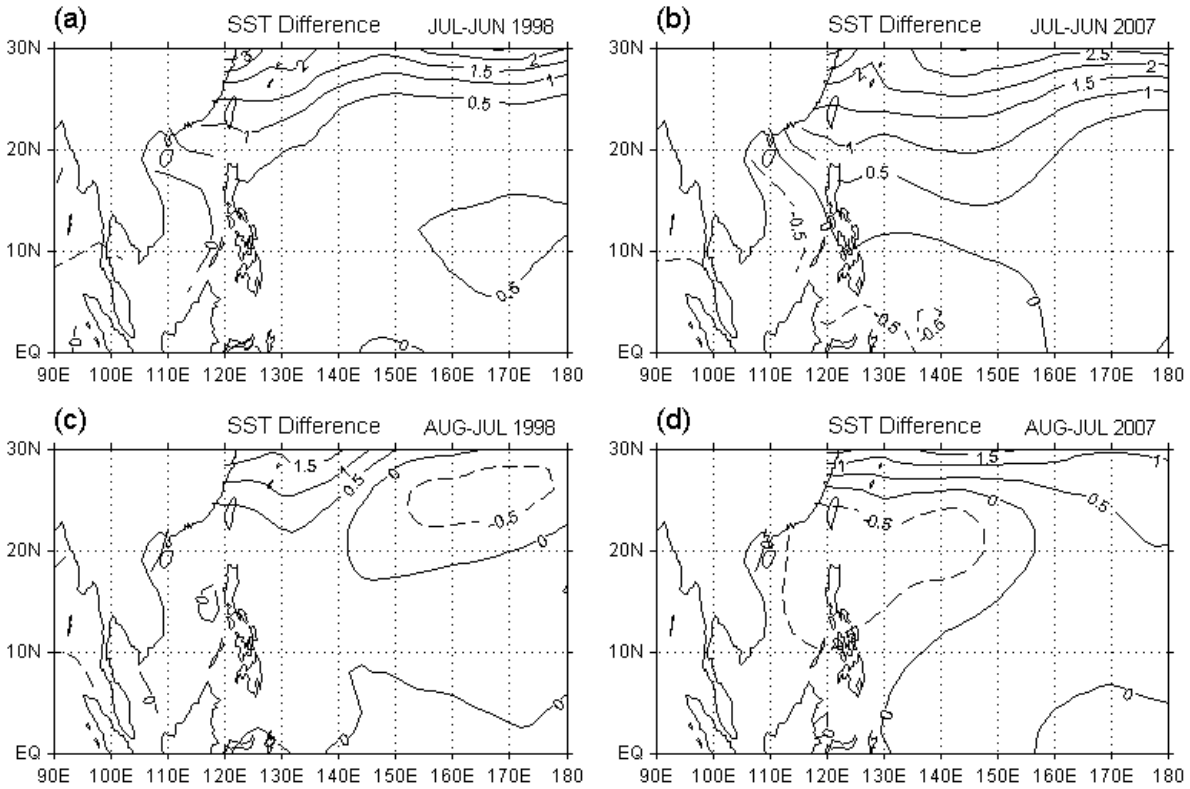
(a)
SST Difference
JUL-JUN 1998
(b)
SST Difference
JUL-JUN 2007
(c)
SST Difference
AUG-JUL 1998
(d)
SST Difference
AUG-JUL 2007
30N
20N
10N
EQ
90E 100E 110E 120E 130E 140E 150E 160E 170E 180

669 Fig. 16

670

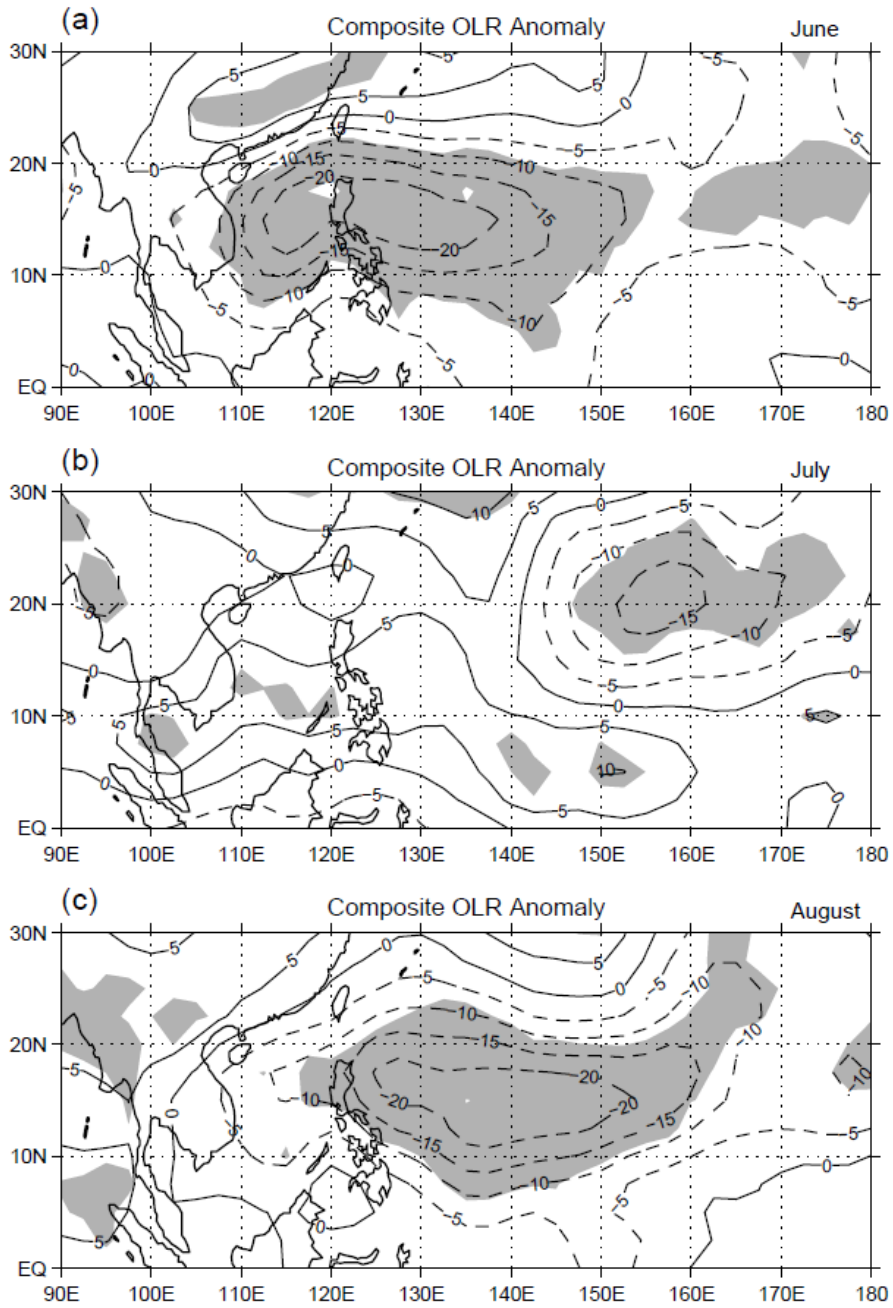

671